ACS OMEGA

http://pubs.acs.org/journal/acsodf

Article

Effect of the Oxygen Concentration and Temperature on Thermal Decomposition of N_2O in an Inert Gas

Jae Geun Yun, Han Min Lee, Gwang Yeol Baik, Ji Yeop Kim, Sang Ji Lee, Min Kyu Jeon, Sang In Keel, and Jung Goo Hong*

Cite This: *ACS Omega* 2021, 6, 30983−30988

Read Online

ACCESS | Metrics & More | Article Recommendations

ABSTRACT: Nitrous oxide (N_2O) is one of the greenhouse gases that contribute to global warming. But, there are few methods for controlling N_2O directly. It is essential to reduce N_2O to solve environmental problems. In this study, we investigate the O_2 concentration dependence of N_2O decomposition under an argon-based gas mixture in a high-temperature thermal reactor. The gas concentrations are calculated using CHEMKIN. The results confirm that more N_2O is converted to N_2 or NO at lower O_2 concentrations. Therefore, the conversion process is hindered by increasing the O_2 concentration. We propose a modified parameter of N_2O decomposition, and it is employed in the CHEMKIN calculations. With the modified parameter, the experimental results are in a similar tendency to the calculated results.

1. INTRODUCTION

Secondary industries based on fossil fuels emit nitrogen oxides. To minimize air pollution, the Kyoto protocol, which controls greenhouse gases, was signed in 1997. Six gases are regulated by the protocol, including carbon dioxide (CO_2), methane (CH_4), hydrofluorocarbons (HFCs), perfluorocarbons (PFCs), sulfur hexafluoride (SF_6), and nitrous oxide (N_2O). Figure 1 shows the global warming potential (GWP) of N_2O

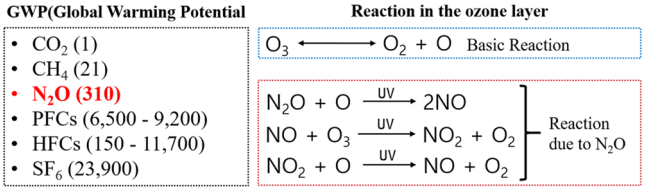

Figure 1. Global warming potential of greenhouse gases and the ozone layer reaction.

and its chemical reaction in the ozone layer. N_2O has a GWP 310 times higher than that of CO_2. It causes chain reactions in the ozone layer and destroys O_3 successively.[1,2] In addition, N_2O takes 135 years to be naturally reduced in the ozone layer. Nevertheless, most OECD (Organization for Economic Cooperation and Development) member countries have considerably insignificant N_2O regulations compared to those of CO_2.[33]

There are a few methods of reducing N_2O emission from stationary sources, such as industrial incinerators or boilers.[4−6] The reduction of N_2O in the exhausts can be divided into two processes: selective catalytic reduction (SCR) and selective noncatalytic reduction (SNCR). SCR can operate at lower temperatures than SNCR, but it has higher maintenance costs than SNCR due to the use of catalysts.

SNCR is a process of reducing NO_x using a reductant without catalysts. It operates at a higher temperature than SCR, but it has a simple structure and low cost of maintenance. NO_x from industrial machines is converted into nitrogen (N_2) and water vapor by injecting a reductant in the exhaust line at temperatures ranging from 1173 to 1373 K.[7] As reductants, ammonia (NH_3) and urea aqueous solutions (urea solution, NH_2CONH_2) are used. A urea solution is easier to manage and cheaper than ammonia.[8,9]

Figure 2 shows the decomposition mechanism and the reaction route of reductants in the SNCR process.[10] The chemical reaction generally follows the Zeldovich mechanism, which explains the oxidation of nitrogen and the formation of NO_x.[11] The mechanism confirms that N_2O is formed inevitably during N_2 conversion from NO_x.[12] Svoboda et al. reported that N_2O formation during the SNCR process is attributed to the reductants.[13]

Received: June 28, 2021
Accepted: October 29, 2021
Published: November 12, 2021

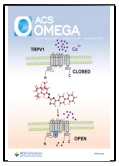

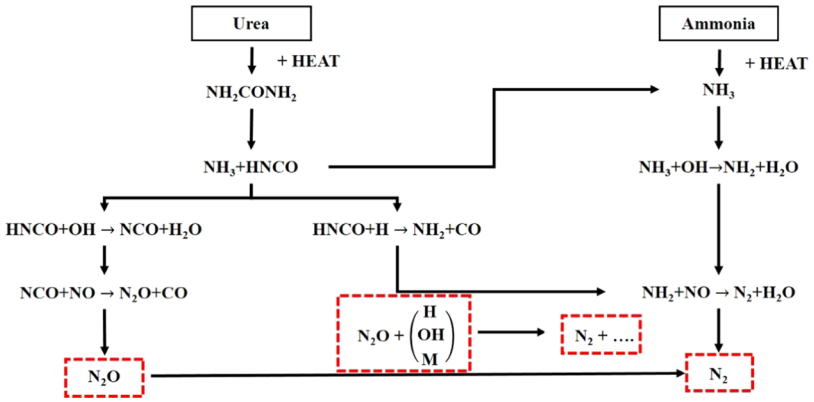

Figure 2. Basic decomposition mechanism of nitrogen oxide under the action of a reductant (photograph was taken by Jae Geun Yun).

Amand et al. reported that N_2O is very sensitive to temperature, and thus, the decomposition mechanism is temperature-dependent.[14] Kilpinen et al. reported that hydrogen cyanide (HCN) is important in the formation of N_2O. HCN is converted to NCO, and N_2O is formed by reacting NCO with NO.[15] Kim reported that N_2O formation in the SNCR process decreases as the O_2 concentration increases.[16] Rahman et al. reported that the temperature range for optimal NO_x-reduction efficiency increases as the O_2 concentration increases.[17] Liu et al. reported that O radicals promote N_2O decomposition.[18] Lee et al. reported that excessive residence time decreases the N_2O reduction efficiency.[19]

Previous studies have shown that N_2O formation during NO_x reduction is affected by the O_2 concentration. However, the dependence of N_2O decomposition on the O_2 concentration has yet not been clarified. In this study, we investigated the reduction of N_2O in varied O_2 concentrations. A laboratory-scale electric furnace was used to simulate the actual SNCR process. Thermal decomposition experiments were conducted to examine the reaction characteristics of Ar-based N_2O mixtures. The temperature of the reactor and the O_2 concentration of the mixture were set as experimental variables. Comparing experimental results with those calculated using CHEMKIN, we propose modified factors for the reaction mechanism and the rate constant of GRI 3.0.

CHEMKIN-PRO software is designed for modeling many chemically reacting flow configurations. Successful application of CHEMKIN-PRO to engineering and chemistry problems requires some basic understanding of the theory and formulations behind chemically reacting flow simulations. The CHEMKIN-PRO Theory Manual provides a broad overview of the relationships and formulations used in calculations of chemical property and source terms. It also provides brief derivations and explanations of the governing equations solved by CHEMKIN-PRO Reactor Models, as well as a discussion of numerical solution techniques and sensitivity analysis employed in the models.

GRI-Mech 3.0 is an optimized mechanism designed to model natural gas combustion, including NO formation and reburn chemistry. It is the successor to version 2.11 and another step in the continuing updating evolution of the mechanism. The optimization process is designed to provide sound basic kinetics, which also furnishes the best-combined modeling predictability of basic combustion properties.

2. RESULTS AND DISCUSSION

2.1. Formation of N_2 and NO by Thermal Decomposition of N_2O. Figure 3 shows the variation of the calculated gas concentrations with the reactor temperature. The gas mixture is composed of 99.96% Ar, 0% O_2, and N_2O (400 ppm). The reactor temperature was varied from 1073 to 1273 K, and the residence time was fixed at 7 s. The N_2O concentration decreased with increasing reactor temperature. At the initial temperature (1073 K), the N_2O concentration was 336 ppm. N_2O was entirely decomposed at 1273 K. The N_2 concentration increased with a decrease in the N_2O concentration, reaching 368 ppm at a reactor temperature of 1273 K. This is attributed to the N_2O thermal decomposition to two N and one O components, according to eq 3 of Table 3. The two N components react again and form stable N_2 molecules. The NO concentration slightly increased with decreasing N_2O concentration. The concentration of NO was very small at the initial temperature (1073 K), but it reached 21 ppm when the reactor temperature was increased to 1273 K. This is attributed to the conversion of N_2O to NO, according to eq 3 of Table 3. Above a reactor temperature of 1240 K, the NO concentration was greater than that of N_2O. Therefore, N_2O thermal decomposition must be conducted under an appropriate level of temperature to avoid excessive NO_x production.

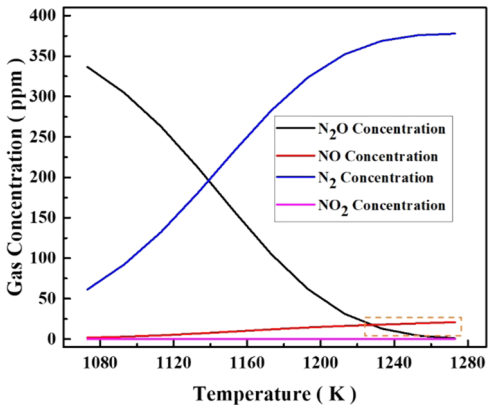

Figure 3. Calculated gas concentration at different temperatures using CHEMKIN.

2.2. N_2O Concentration Depending on the O_2 Concentration. Figure 4 shows the variation of the N_2O concentration with reactor temperatures and O_2 concen-

https://doi.org/10.1021/acsomega.1c03365
ACS Omega 2021, 6, 30983−30988

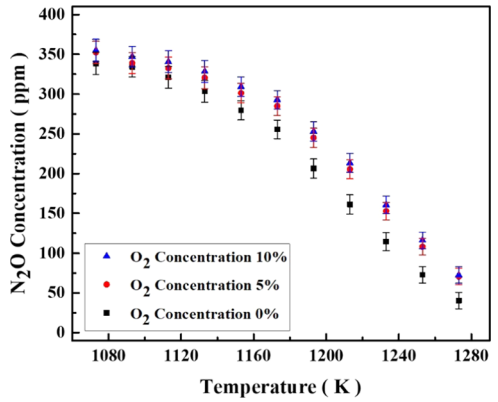

Figure 4. N_2O concentration according to O_2 in the experiment.

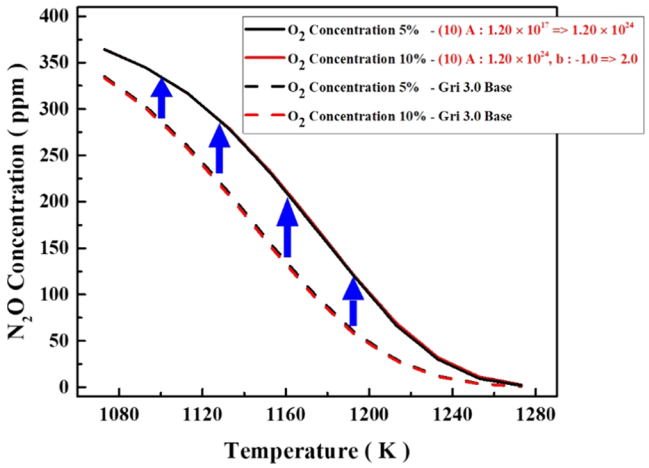

Figure 5. N_2O concentration according to O_2 in comparison with the modified parameter and the GRI 3.0 mechanism.

trations. The gas mixture compositions are listed in Table 2. The reactor temperature was varied from 1073 to 1273 K, and the residence time was fixed at 7 s. The N_2O curves were varied with the O_2 concentration in the gas mixture. For all three gas compositions, the N_2O concentration decreased with increasing temperature, but the concentration of N_2O for each temperature increased with increasing O_2 concentration. This is attributed to the conversion of N_2O to N_2 and NO with a lower O_2 concentration, following eqs 1−3 of Table 1.

2.3. Calculated N_2O Concentration with the Modified Parameter Constant. Figure 5 shows the variation of the calculated N_2O concentration with temperature using the GRI 3.0 and the modified parameter. O_2 concentrations of 5 and 10% were employed for each mechanism. In the case of a 0% O_2 concentration, eq 10 is considered insignificant, thus the GRI 3.0 mechanism was used for the calculation. For the modified parameter, only the value of A was varied from 1.20×10^{17} to 1.20×10^{24} $(cm^3/gmol)/s$ at 5% O_2. However, both A and b were varied to 1.20×10^{24} $(cm^3/gmol)/s$ and 2.0, respectively, at 10% O_2. The parameter of the GRI 3.0 mechanism was modified because it has different experimental environments and purposes. The GRI 3.0 mechanism is designed for calculating the natural gas combustion, NO formation, and reburn chemistry. The main proposal of this paper is to study the thermal decomposition and reaction analysis of N_2O based on an Ar atmosphere, which is different from natural gas (CH_4). In addition, while a real combustion reaction and flow rate are fast, the gas mixture of the experiment reacts slowly because the velocity of the flow is only 10.7 cm/s. Therefore, to increase effective collisions, the values of A (a frequency or pre-exponential factor) and b (temperature proportional constant) were modified in the GRI-Mech 3.0. That is, as A in the reaction equation increases, the reaction occurs more easily. In this study, A and b values were modified to compare with actual experimental results. In addition, although modifications of the variables in eqs 1−8 were endlessly attempted, there was no significant change according to the oxygen concentration. But, in modification of eq 8, there clearly was a difference according to the oxygen concentration. For example, b and E_a were fixed, and the A value was calculated as 10^{17}, 10^{18}, 10^{19}, and 10^{20} $(cm^3/gmol)/s$. Also, A and E_a were fixed, and the b value was calculated as −2, −1, 0, 1, 1.5, and 2. Finally, we suggest that the parameter was optimized for experimental results.

The factors of the rate constant were modified to verify the reactants or the decomposition mechanism. Comparing the calculated data, the modified parameter increased the N_2O concentration by 30 ppm relative to that of the GRI 3.0 mechanism at the same O_2 concentration and temperature.

Figure 6 shows the variation of the experimental and calculated N_2O concentrations with temperature. The compositions of the experimental gas mixture are listed in Table 1. The calculation was conducted using the modified parameter, as shown in Figure 5. The calculated results show a decrease in N_2O for all O_2 concentrations as temperature increases. The graph curve of a decreasing trend of the calculated data was similar to the experimental data depending on the O_2 concentration. In the calculations results, the conversion of N_2O to N_2 or NO increases with decreasing O_2 concentration. In the case of a 0% O_2 concentration, eq 8 is considered insignificant, thus the GRI 3.0 mechanism was used

Table 1. Elementary Reaction of N_2O (the Modified Parameter)

	$k = AT^b \exp(-E_a/RT)$		
reaction	A $(cm^3/gmol)/s$	b	E_a (kJ/gmol)
$N_2O(+M) <=> N_2 + O(+M)$(1)	7.9×10^{10}	0	56 020
$N_2O + O <=> N_2 + O_2$(2)	1.4×10^{12}	0	10 810
$N_2O + O <=> 2NO$(3)	2.9×10^{13}	0	23 150
$NO_2 + O <=> NO + O_2$(4)	3.9×10^{12}	0	−240
$NO + O + M <=> NO_2 + M$(5)	1.06×10^{20}	−1.41	0
$N + NO <=> N_2 + O$(6)	2.7×10^{13}	0	355
$N + O_2 <=> NO + O$(7)	9.0×10^{9}	1	6500
$2O + M <=> O_2 + M$(8)	1.20×10^{24}	2.00	0

https://doi.org/10.1021/acsomega.1c03365
ACS Omega 2021, 6, 30983−30988

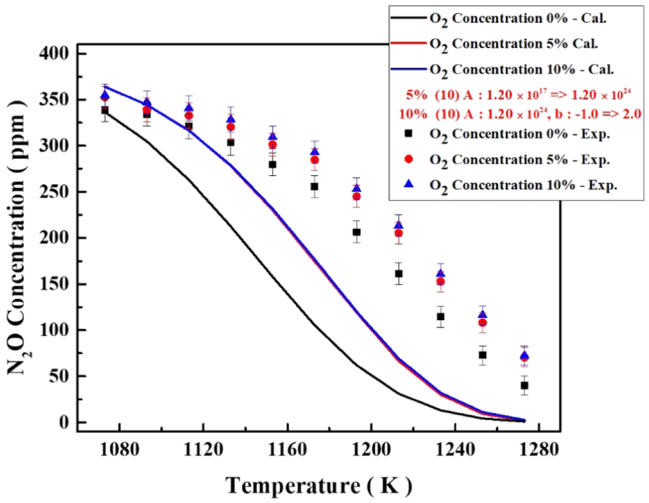

Figure 6. N_2O concentration according to O_2 in comparison of calculation and experimental results.

for the calculations. At 0% O_2, the N_2O concentration was 336, 105, and 0 ppm at 1073, 1173, and 1273 K, respectively. The experimental results show a similar tendency with that of the modified parameter. There are intervals between the experimental values and the calculated values because of the insulation conditions and the ideal gas behavior model.

3. CONCLUSIONS

In this study, we investigated the effect of the O_2 concentration and temperature on the thermal decomposition of N_2O. GRI 3.0 and the modified parameter were verified by comparing the calculated and experimental results. The major findings of this work are summarized as follows:

(1) Through calculation, it was confirmed that N_2O is critically affected by temperature. The N_2O concentration decreases according to an increase in temperature. Also, it was confirmed that N_2O molecules were converted to N_2 and NO by eqs 1−3.

(2) As a result of the N_2O thermal decomposition experiment according to the temperature, N_2O decreases according to an increase in temperature. Also, it was confirmed that the more oxygen there is, the more it interferes with the decomposition of N_2O. Higher O_2 concentrations are attributed to the increase in the decomposition reaction of N_2O.

(3) The calculation using GRI 3.0 showed little difference in the N_2O concentration depending on the oxygen concentration, but the calculation using the modified parameters showed that the best reduction in the oxygen concentration was 0%. Therefore, with the modified parameter, the graph curve of the decreasing trend of the calculated data was similar to the experimental data depending on the O_2 concentration.

(4) There was a gap between the experimental and calculated results regardless of GRI 3.0 Base and modified parameter GRI 3.0, but the difference was not important in this study. The reason for the gap was assumed to be because of the PFR model of ideal flow and heat loss from the reactor.

4. MATERIALS AND METHODS

4.1. Experimental Setup. Figures 7 and 8 show a schematic diagram and a picture, respectively, of a laboratory-scale electric furnace reactor for N_2O thermal decomposition. The experimental apparatus comprises a gas supply unit, a thermal reactor, a measurement device, and an emission part. Experimental gases (Ar, O_2, and N_2O) flow through a mass flow controller (MFC).

The thermal reactor is a cylindrical tube (inner diameter: 114 mm; length: 750 mm) and can be heated up to 1373 K using three internal heating coils. An insulator surrounds the reactor to prevent heat loss and maintain the temperature of the experiment. The temperature of the reactor was measured using R-type thermocouples.[20] Here, the concentration of the exhaust gas after the reaction was measured using a nondispersive infrared (NDIR) gas meter (NOVA IR-Pro). The measurement error of the gas meter was below 2% (electrochemical sensor).

4.2. Experimental Conditions. Table 1 shows the test gas conditions for the thermal decomposition experiment. The gas mixture was composed of Ar (89.96−99.96%), O_2 (0−10%), and N_2O (400 ppm). The actual combustion exhaust gas was N_2 and CO_2. The Ar-based mixture was used to investigate the separate thermal reaction of N_2O. The residence time of the experimental gas in the thermal reactor was fixed at 7 s. NO_x and N_2O production depends on the O_2 concentration and temperature. Thus, the O_2 concentration of the gas mixture and the reactor temperature were varied during the experi-

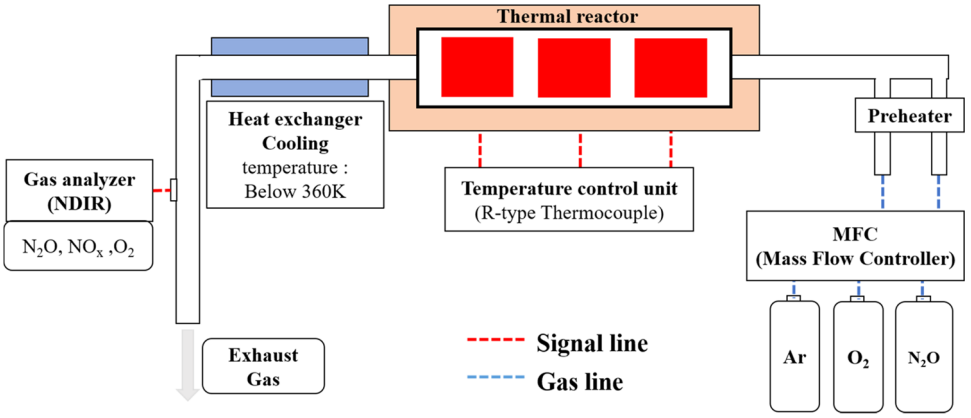

Figure 7. Schematic diagram of the experimental setup (photograph was taken by Jae Geun Yun).

https://doi.org/10.1021/acsomega.1c03365
ACS Omega 2021, 6, 30983−30988

Figure 8. Laboratory-scale selective noncatalytic reduction (SNCR) system (photograph courtesy of Sang Ji Lee. Copyright 2021).

Table 2. Test Gas Conditions

residence time (s)	gas composition
7	Ar (99.96%), O_2 (0%), N_2O (400 ppm)
	Ar (94.96%), O_2 (5%), N_2O (400 ppm)
	Ar (89.96%), O_2 (10%), N_2O (400 ppm)

Table 3. Experimental Conditions

condition	value
temperature (K)	1073−1273
flow rate (L/min)	18.34−15.46
ambient temperature (K)	298
ambient pressure (atm)	1

ment. The O_2-concentration dependence of N_2O thermal decomposition was investigated by varying the O_2 composition of the gas mixture at fixed residence times. The gas mixture flow rate was calculated using eq 9. In this equation, Q is the gas flow rate, D is the inner diameter of the reactor, L is the length of the reactor, and t is the residence time.

$$Q = \frac{\pi \times (D/2)^2 \times L}{t} \tag{9}$$

Table 2 shows the experimental conditions. Considering the normal SNCR temperature, the experimental temperature ranged from 1073 to 1273 K at a 20 K interval. For a fixed residence time of the gas mixture at each temperature, the flow rate was varied according to Charles' law, expressed as follows

$$\frac{Q_1}{T_1} = \frac{Q_2}{T_2} \tag{10}$$

where Q_1 is the inlet flow rate, T_1 is the inlet temperature, Q_2 is the flow rate for each temperature, and T_2 is the reactor temperature. The concentration of the exhaust gas was measured in a 1 min interval at the rear end of the reactor after 15 min of gas supply. The numerical and graphical data reported here are the average values of 110 measurements for each experimental condition. Ambient conditions were maintained in atmospheric air (298 K, 1 atm). In high-temperature plasma, the recombination of O_2 atoms in the presence of a third body M is prominent. The asterisk on M in the stoichiometric equation indicates that M is energized in the reaction.

4.3. CHEMKIN Calculation Conditions. The N_2O thermal decomposition was simulated using CHEMKIN.[21] A one-dimensional (1D) plug flow reactor (PFR) model was employed in the simulations. The PFR model is a cylindrical reactor model that assumes a steady state during flow. The inlet gas was assumed to be perfectly mixed, therefore, continuous thermal reactions were observed inside the reactor. The furnace model has an inner diameter of 114 mm and a length of 750 mm, which is the same as the experimental setup. The temperature of the reactor was divided into 11 sections, ranging from 1073 to 1273 K. The residence time of the gas mixture was set as 7 s, considering the actual experimental conditions. The N_2O chemical reaction was calculated from the GRI 3.0[22] and reaction equations in Tables 3 and 4.

Table 4. Elementary Reaction of N_2O (GRI 3.0 Base)

	$k = AT^b \exp(-E_a/RT)$		
reaction	A (cm^3/gmol)/s	b	E_a (kJ/gmol)
$N_2O(+M) <=> N_2 + O(+M)$ (1)	7.9×10^{10}	0	56 020
$N_2O + O <=> N_2 + O_2$ (2)	1.4×10^{12}	0	10 810
$N_2O + O <=> 2NO$ (3)	2.9×10^{13}	0	23 150
$NO_2 + O <=> NO + O_2$ (4)	3.9×10^{12}	0	−240
$NO + O + M <=> NO_2 + M$ (5)	1.06×10^{20}	−1.41	0
$N + NO <=> N_2 + O$ (6)	2.7×10^{13}	0	355
$N + O_2 <=> NO + O$ (7)	9.0×10^{9}	1	6500
$2O + M <=> O_2 + M$ (8)	1.20×10^{17}	−1.00	0

https://doi.org/10.1021/acsomega.1c03365
ACS Omega 2021, 6, 30983−30988

$$k = AT^{b} \exp(-E_a/RT) \quad (11)$$

Equation 11 is the modified Arrhenius equation, where k is the rate constant. It can be used as an objective index indicating the characteristics of the chemical reaction rate. The rate of a chemical reaction can be varied using catalysts, which change the activation energy and the reaction route. The rate constant and activation energy are closely related. The rate constant of a reaction depends on the reaction temperature. The reaction rate increases with an increase in temperature due to the increase in the rate constant. In eq 11, A is a frequency or pre-exponential factor, b is a temperature proportional constant, E_a is the activation energy, R is the gas constant, and T is the absolute temperature.

AUTHOR INFORMATION

Corresponding Author

Jung Goo Hong − *School of Mechanical Engineering, Kyungpook National University, Daegu 41566, Republic of Korea*; Phone: 82-53-950-6570; Email: jghong70@knu.ac.kr; Fax: 82-53-950-6550

Authors

Jae Geun Yun − *School of Mechanical Engineering, Kyungpook National University, Daegu 41566, Republic of Korea*

Han Min Lee − *School of Mechanical Engineering, Kyungpook National University, Daegu 41566, Republic of Korea*

Gwang Yeol Baik − *School of Mechanical Engineering, Kyungpook National University, Daegu 41566, Republic of Korea*

Ji Yeop Kim − *School of Mechanical Engineering, Kyungpook National University, Daegu 41566, Republic of Korea*

Sang Ji Lee − *School of Mechanical Engineering, Kyungpook National University, Daegu 41566, Republic of Korea*

Min Kyu Jeon − *Department of Environmental Machinery, Korea Institute of Machinery & Materials, Daejeon 34103, Republic of Korea*

Sang In Keel − *Department of Environmental Machinery, Korea Institute of Machinery & Materials, Daejeon 34103, Republic of Korea*

Complete contact information is available at: https://pubs.acs.org/10.1021/acsomega.1c03365

Author Contributions

H.M.L., G.Y.B., J.Y.K., S.J.L., M.K.J., and S.I.K. contributed to conceptualization, methodology, software, validation, and data curation; J.G.Y. contributed to writing—original draft preparation; S.I.K. and J.G.H. contributed to writing—review and editing; and J.G.H. contributed to supervision. All authors have read and agreed to the published version of the manuscript.

Funding

National Research Council of Science & Technology (NST) grant by the Korean government (MSIP) (No. CRC-15-07-KIER).

Notes

The authors declare no competing financial interest.

ACKNOWLEDGMENTS

This research was supported by the Technology Development Program to Solve Climate Changes through the National Research Council of Science & Technology (NST) grant by the Korean government (MSIP) (No. CRC-15-07-KIER).

REFERENCES

(1) Chang, K. S. Status and Trends of Emission Reduction Technologies and CDM Projects of Greenhouse Gas Nitrous Oxide. *J. Korean Ind. Eng. Chem.* **2008**, *19*, 17−26.

(2) Choi, S. H.; Ko, J. C. Investigation of N_2O Emission Characteristics and Emission Factors of Solid Fuel Incineration Facilities. *J. Korean Soc. Environ. Eng.* **2019**, *41*, 82−88.

(3) Yoon, I. J. In *Key Issues and Prospects of the Paris Agreement*, Law Research Institute Summer Joint Conference, 2017; pp 113−144.

(4) Jeon, S. G. N_2O Reduction Technology and Catalyst Research and Development Trend. *Ind. Chem. Outlook* **2016**, *19*, 33−44.

(5) Cooper, C. D.; Alley, F. C. *Air Pollution Control: a Design Approach*; Waveland Press, 1994, pp 488−497.

(6) Gullet, B. K.; Paul, W. G.; Lin, M. L.; James, M. C. NO_x Removal with Combined Selective Catalytic Reduction and Selective Non Catalytic Reduction: Pilot-Scale Test Results. *J. Air Waste Manage. Assoc.* **1994**, *44*, 1188−1194.

(7) Jang, J. H. Removal of NO_x in SNCR Process Using Urea and Additives, Master's Thesis; School of Environmental Engineering, The University of Seoul, 2003.

(8) Østberg, M.; Kim, D. J.; Johnsson, J. E. Influence of Mixing on the SNCR process. *Chem. Eng. Sci.* **1997**, *52*, 2511−2525.

(9) Oxley, J. C.; Smith, J. L.; Rogers, E.; Yu, M. Ammonium nitrate: Thermal Stability and Explosivity Modifiers. *Thermochim. Acta* **2002**, *384*, 23−45.

(10) Smith, R. A.; Muzio, L. J.; Hunt, T. *Integrated Dry NO_x/SO_2 Emissions Control System: Low-NO_x Combustion System SNCR Test Report*, Public service company of Colorado, DOE: DE-FC22-91PC90550, 1997.

(11) Zeldovich, Y. B.; Barenblatt, G. I.; Librovich, V. B.; Makhviladze, G. M. *The Mathematical Theory of Combustion and Explosion*; Plenum Press, 1985; p 597.

(12) Jung, M. S. A Study on the Reduction of N_2O generation at SNCR Process Using Urea and Additives, Master's Thesis; School of Environmental Engineering, The University of Seoul, 2011.

(13) Svoboda, K.; Baxter, D.; Martinec, J. Nitrous Oxide Emissions from Waste Incineration. *Chem. Pap.* **2006**, *60*, 78−90.

(14) Amand, L.; Andersson, S. In *Emissions of Nitrous Oxide from Fluidized Bed Boilers*, International Conference on Fluidized Bed Combustion; 1989; pp 49−56.

(15) Kilpinen, P.; Mikko, H. Homogeneous N_2O Chemistry at Fluildized Bed Combustion Conditions: A Kinetic Modeling Study. *Combust. Flame* **1991**, *85*, 94−104.

(16) Kim, J. M. A Study on the Reduction Mechanism of NO_x and N_2O in Urea-SNCR Process, Master's Thesis; School of Environmental Engineering, The University of Seoul: Seoul, 2012.

(17) Rahman, Z. U.; Wang, X.; Zhang, J.; Jakov, B.; Millan, V.; Tan, H. Kinetic Study and Optimization on SNCR Process in Pressurized oxy-Combustion. *J. Energy Inst.* **2021**, *94*, 263−271.

(18) Liu, S. L.; Fan, W. D.; Shen, P. H.; Wu, X. F.; Chen, J.; Guo, H. The Effect of Iodine Additive and Char on the Heterogeneous Decomposition of N_2O and the Generation of NO under High Temperature. *Fuel* **2019**, *256*, No. 115949.

(19) Lee, H. M.; Yun, J. G.; Hong, J. G. A Study of Nitrous Oxide Thermal Decomposition and Reaction in High Temperature Inert Gas. *J. ILASS-Korea* **2020**, *25*, 132−138.

(20) Lee, S. J.; Yun, J. G.; Lee, H. M.; Kim, J. Y.; Yun, J. H.; Hong, J. G. Dependence of N_2O/NO Decomposition and Formation on Temperature and Residence Time in Thermal Reactor. *Energies* **2021**, *14*, No. 1153.

(21) CHMEKIN-PRO, Reaction Design Inc, San Diego, CA 92121, USA, https://www.Ansys.com/.

(22) Smith, G. P.; Golden, D. M.; Frenklach, M.; Moriarty, N. W.; Eiteneer, B.; Goldenberg, M.; Bowman, C. T.; Hanson, R. K.; Song, S.; Gardiner, W. C., Jr.; Lissianski, V.; Qin, Z. http://www.me.Berkeley.Edu/GRI_Mech/.

https://doi.org/10.1021/acsomega.1c03365
ACS Omega 2021, 6, 30983−30988